

A Dedicated M-Dwarf Planet Search Using The Hobby-Eberly Telescope ¹

Michael Endl, William D. Cochran, Robert G. Tull
and

Phillip J. MacQueen

McDonald Observatory, The University of Texas at Austin, Austin, TX 78712, USA

mike@astro.as.utexas.edu; wdc@astro.as.utexas.edu; rgt@astro.as.utexas.edu;
pjm@astro.as.utexas.edu

ABSTRACT

We present first results of our planet search program using the 9.2 meter Hobby-Eberly Telescope (HET) at McDonald Observatory to detect planets around M-type dwarf stars via high-precision radial velocity (RV) measurements. Although more than 100 extrasolar planets have been found around solar-type stars of spectral type F to K, there is only a single M-dwarf (GJ 876, Delfosse et al. 1998; Marcy et al. 1998; Marcy et al. 2001) known to harbor a planetary system. With the current incompleteness of Doppler surveys with respect to M-dwarfs, it is not yet possible to decide whether this is due to a fundamental difference in the formation history and overall frequency of planetary systems in the low-mass regime of the Hertzsprung-Russell diagram, or simply an observational bias. Our HET M-dwarf survey plans to survey 100 M-dwarfs in the next 3 to 4 years with the primary goal to answer this question. Here we present the results from the first year of the survey which show that our routine RV-precision for M-dwarfs is 6 m s^{-1} . We found that GJ 864 and GJ 913 are binary systems with yet undetermined periods, while 5 out of 39 M-dwarfs reveal a high RV-scatter and represent candidates for having short-periodic planetary companions. For one of them, GJ 436 ($\text{rms} = 20.6 \text{ m s}^{-1}$), we have already obtained follow-up observations but no periodic signal is present in the RV-data.

Subject headings: stars: late-type — stars: low mass — planetary systems — techniques: radial velocities

1. Introduction

M-dwarf stars form the majority of stars in our galaxy, both in numbers as well as in total mass. However, Doppler surveys looking for stellar reflex motions due to planetary companions via precise radial velocity measurements, have traditionally focused on the brighter F,G and K-type stars in order to obtain a sufficient signal-to-noise ratio of the high resolution (typically $R > 50,000$)

spectra. This has led to the discovery of more than 100 extrasolar giant planets orbiting solar-type stars (Mayor & Queloz 1995, see e.g. Fischer et al. 2003 for recent detections). Due to their intrinsic faintness and thus need of large aperture telescopes, M dwarfs constitute only a small fraction of the target-samples of these surveys. Up to now, there is only a single M-dwarf, GJ 876 (M4V, $M=0.3 M_{\odot}$), known to possess a planet with a minimum mass of $m \sin i \approx 2 M_{\text{Jup}}$ in a 60 day orbit (Delfosse et al. 1998; Marcy et al. 1998). Follow-up observations revealed the presence of a second companion with $m \sin i = 0.56 M_{\text{Jup}}$ moving in a 2:1 mean motion resonance (Marcy et al. 2001). In combination with the RV data Benedict et al. (2002) used the HST Fine Guidance

¹Based on data collected with the Hobby-Eberly Telescope, which is operated by McDonald Observatory on behalf of The University of Texas at Austin, the Pennsylvania State University, Stanford University, Ludwig-Maximilians-Universität München, and Georg-August-Universität Göttingen.

Sensors (FGS) to measure the astrometric perturbation of GJ 876 caused by the outer planet, and thus to determine the orbital inclination and the true mass of the companion.

There were few attempts to target specifically M-dwarfs to look for substellar companions. Starting in 1995 the Delfosse et al. (1999) Doppler survey monitors a volume-limited sample of 127 M-dwarfs with the ELODIE spectrograph at Observatoire de Haute-Provence and the CORALIE instrument at ESO La Silla. Their long-term RV-precision spans from 10 m s^{-1} for the brighter stars to 70 m s^{-1} for the fainter objects. Beside the planetary companion to GJ 876, they also discovered several spectroscopic stellar binary systems in their sample (Delfosse et al. 1999). The Keck Doppler survey of the Berkeley group includes ≈ 150 M-stars and they achieve a long-term RV precision of $3-4 \text{ m s}^{-1}$ (Vogt et al. 2000). The Keck Hyades program of Cochran et al. (2002) also contains a subsample of 20 M-stars. In the southern hemisphere we have been using the ESO VLT and the UVES spectrograph to observe 25 M-stars for 2 years now. The high RV precision and sampling density we obtain for Proxima Cen (M5V) would have already allowed us to detect very low-mass planets ($m \sin i = 0.0126 - 0.019 M_{\text{Jup}}$ or $m \sin i = 4 - 6 M_{\oplus}$) inside the habitable zone of that star (Endl et al. 2003), while in the case of Barnard’s star (M4V) we successfully measured the secular acceleration of the RV for the first time and discovered a correlation between our RV data and the $\text{H}\alpha$ emission level for this M-dwarf (Kürster et al. 2003).

With the exception of the Delfosse et al. and our VLT program, none of the above mentioned surveys aim for M-dwarfs as primary targets and in general low-mass stars constitute only a subsample of larger targetlists. Our HET program only observes M-dwarfs, since we are especially interested in the prevalence of planetary systems in this section of the HR-diagram.

2. Planets around M-dwarfs

M-dwarfs form the majority of stars in our galaxy, both in total numbers as well as in cumulative mass. Knowledge about the properties and frequency of planetary systems for this type of stars would therefore have vast implications on

the overall statistics of planetary companions in the galaxy.

So far no detailed physical models for planet formation in general or as a function of stellar mass in particular are available. To our knowledge, Nakano (1988) was the first to study planet formation timescales for stars of varying mass and lifetimes. Wetherill (1996) simulated the formation of terrestrial planets for stars of different mass and disks of different surface densities, and found that the end-products of planetesimal accretion are rather insensitive to the stellar mass. However, the low-mass star chosen in both studies has a mass of $0.5 M_{\oplus}$, which is the high end of the M-dwarf mass distribution. Since formation of gas giant planets is even less understood (it is not clear yet whether jovian planets form in a “bottom-up” process, i.e. by gas accretion onto a rocky core of $\approx 10 M_{\oplus}$ (e.g. Pollack et al. 1996), or by a type of gravitational disk instabilities leading to a “top-down” collapse and rapid formation of the gas giant without the need of a rocky core (e.g. Boss 1997), reliable theoretical predictions on the frequency of planetary systems depending on initial conditions like stellar primary and disk mass as well as disk composition are difficult to make.

Therefore, our goal is to obtain a useful statistical overview of planetary systems in the M-dwarf regime by observational means. In the near future we will know if GJ 876 remains a special case or if more planets around M-dwarfs will be detected by our survey or one of the other programs.

3. The HET survey and radial velocity results

Table 1 lists 35 targets (out of a total of 39, 4 candidate objects for short-periodic companions are not listed) of our survey, the total rms-scatter of their RV-data and the duration of monitoring. With a few exceptions the short time span of observations limits our detection capability to short-periodic planets with periods of a few days. Extension of the time baseline will allow us to become sensitive also to longer period planets at larger orbital separations.

All targets were selected based on the Gliese catalogue of nearby stars (Gliese & Jahreiß 1991) and the Hipparcos astrometric database (ESA 1997). In order to minimize the effects of stellar activity

on our RV measurements (especially rotational modulation by star spots) we choose only targets with no detected or low X-ray emission using the ROSAT all-sky survey results from Hünsch et al. (1999).

In our observing strategy we usually first take 5 RV measurements per target over a short time to test for short-periodic variability. If variability is detected the same target will be re-scheduled for more intense monitoring. Seemingly constant stars will be re-observed later in our survey and with a longer cadence in order to check for long-term variability (companions at larger orbital separations).

This work presents the first results our program, which we plan to continue until we have sampled ≈ 100 M-dwarfs with the necessary RV-precision to find orbiting giant and lower mass giant planets.

For the observations we use the HET High-Resolution-Spectrograph (HRS; Tull 1998) which is located in an insulated chamber below the telescope. An optical fiber connects the instrument to the prime focus of the HET and also provides excellent scrambling of the light beam in order to isolate the spectrograph from variations in the telescope pupil illumination. All spectra of our program are taken at a resolving power of $R = 60,000$ and an I_2 cell is inserted into the light path for self-calibration purposes.

3.1. RV-precision

To extract the Doppler shift information from the M-dwarf spectra with the superimposed iodine vapor (I_2) reference spectrum we perform a full data modeling including the reconstruction of asymmetries of the instrumental profile (IP) at the time of observation. In this modeling scheme we subdivide the spectrum into smaller segments and establish a best-fit model, based on a stellar template spectrum of the target and a laboratory spectrum (a Fourier Transform Spectrometer scan) of the I_2 cell, for each segment. The RV of the target is measured differentially to the template while the dense forest of superimposed I_2 lines delivers the wavelength calibration and the information to reconstruct the IP. The uncertainty of the RV measurement is determined from the overall scatter of all segments along a spectrum. A detailed de-

scription of this technique can be found in Butler et al. (1996) and Endl, Kürster, Els (2000).

Fig. 1 shows the histogram of our RV-results. The bulk of the distribution on the left side consists of the M-dwarfs, which are either constant within our measurement precision or their residuals after subtraction of RV-trends do not reveal additional scatter (GJ 623, GJ 708, GJ 864 and GJ 913). Fitting a Gaussian to this part of the histogram yields a mean value of 5.7 m s^{-1} with $\sigma = 2.2 \text{ m s}^{-1}$, which is our present mid-term RV-precision for stars in the magnitude range of $V = 9 - 11 \text{ mag}$ (with the bright ($V = 7.5$) M2V star GJ 411 being the sole exception). The right-hand “tail” of the RV-scatter distribution contains low-amplitude variable stars (all with rms $> 10 \text{ m s}^{-1}$), which we want to sample more frequently to check for short-periodic planetary companions as possible cause of the higher RV-scatter.

There are several sources which contribute to the RV-distribution seen in Fig. 1: 1. intrinsic variability of the targets (i.e. activity induced “RV-jitter” or Keplerian motion due to unknown substellar or stellar companions), 2. the photon noise, 3. the stability of the spectrograph used for the RV measurements, and 4. “algorithmic noise” introduced during the data modeling process (e.g. inadequate characterization of the instrumental profile and imperfect stellar template deconvolution). For the M-dwarf HET sample we conclude that photon noise is the major contributor to the RV-scatter. For earlier type stars of visual magnitude of $V \approx 7 \text{ mag}$, using the same instrumental setup and analysis technique, we obtain a routine long-term RV-precision of $\approx 3 \text{ m s}^{-1}$ (Cochran et al. 2003), a factor 2 better than for the fainter M-dwarfs.

3.2. RV-results

The RV-results of all targets listed in table 1 are displayed in Fig. 2 to Fig. 10. To allow a better comparison we plot all results on the same velocity scale (-30 m s^{-1} to $+30 \text{ m s}^{-1}$), with the exception of GJ 436 (Fig. 6) where the scale is enlarged. For GJ 623, GJ 748, GJ 864 and GJ 913 we show the RV-data after subtraction of a large amplitude RV trend (see section 3.3).

For one of the targets in the high-rms part of the distribution, GJ 436, we have already obtained

follow-up observations (see Fig. 6). A search for periodic signals using the Lomb-Scargle periodogram (Lomb 1976, Scargle 1982) did not reveal any significant signal in the power spectrum (the highest peak has a false-alarm-probability of 32%). The X-ray luminosity of $L_X = 0.7 \times 10^{27} \text{ erg s}^{-1}$ (Hünsch et al. 1999) might point toward stellar activity as cause of the excess scatter. However, GJ 411 with a similar level of coronal emission ($L_X = 0.6 \times 10^{27} \text{ erg s}^{-1}$) and GJ 272 with $L_X = 3.1 \times 10^{27} \text{ erg s}^{-1}$ the brightest X-ray source in our sample, do not show an increased RV-scatter. The cause of the variability of GJ 436 hence remains unknown. The other variable targets are currently in the observing queue of the HET and are pending re-observations.

3.3. Linear and non-linear RV trends

Three targets of our sample are either previously known (GJ 623, GJ 748) or suspected (GJ 913) binary stars.

GJ 623 was found to be an astrometric binary by Lippincott & Borgman (1978) with the latest published value for the orbital period of 3.7 yrs (Nidever et al. 2002). Our HET RV-results are shown in Fig. 11 along with a parabolic fit to the data. Fig. 7 displays the RV-residuals after subtraction of this trend. This data-set is now being used to further improve the binary orbital solution and, in combination with HST FGS astrometry, to accurately determine the masses of the components of the GJ 623 system (Benedict priv. communication).

GJ 748 is another astrometric binary star (Harrington 1977), where we only see a small fraction of the $P = 2.45$ yrs (Franz et al. 1998) orbit (Fig. 12). The residual scatter around a parabolic fit is 5.5 m s^{-1} (Fig. 9).

The entry of GJ 913 in the Hipparcos catalogue contains a double/multiple system annex flag X (stochastic model), which is a hint that the star is actually a short-periodic binary. The HET RV-data (Fig. 13) reveal a large amplitude variation with a Dopplershift of $\approx 500 \text{ m s}^{-1}$ over the time span of 20 days, indicative of binary orbital motion with an unknown period and thus confirming the Hipparcos results. Further observations will allow us to determine a spectroscopic orbit for this star.

In the case of GJ 864 we discovered a linear ac-

celeration in the first 5 RV measurements. Since GJ 864 is not a known (or suspected) binary star and was classified as an RV-constant star in the CORAVEL survey (Tokovinin 1992), we immediately re-scheduled GJ 864 for follow-up observations. As can be seen in Fig. 14 the linear RV-trend continued until the star became unobservable by the HET in December 2002. Using auxiliary RV measurements with the McDonald 2.7 meter telescope in January 2003 we found that the RV-trend of GJ 864 remained linear without any sign of curvature and thus the best explanation for the RV-data is a stellar companion at yet undetermined separation.

4. Discussion

So far, we have found 5 stars out of a sample of 39 M-dwarfs which show a higher RV-scatter than the rest of the sample and which we plan to monitor intensively in the near future to check if the cause of the variability are short-periodic planetary companions. For GJ 436, the one target for which we already obtained follow-up observations, we could not find a periodic signal in the RV-data and the cause of variability remains unknown.

Two stars of our sample turned out to be previously unknown binary stars: GJ 864 and GJ 913. For both targets we soon might be able to establish a spectroscopic orbital solution.

Despite their faintness M-dwarfs hold the promise to detect lower mass extrasolar planets than what is usually possible by precise Doppler surveys. Due to the lower stellar primary mass even planets with the mass of Neptune or lower become detectable in short-periodic orbits. For instance, a planet with $m \sin i = 17 M_{\oplus}$ in a 4 day orbit induces an RV semi-amplitude of $\approx 11 \text{ m s}^{-1}$ on an M0V ($0.5 M_{\odot}$) star, a 2σ -signal for our program. For later M-dwarfs these detection limits approach the terrestrial planet regime as demonstrated by the mass-limits for Proxima Cen (Endl et al. 2003) and Barnard's star (Kürster et al. 2003). Thus, for the time being only precise Doppler monitoring of these low-mass stars has the capability to detect planets with masses below $10 M_{\oplus}$. Supposedly, such low-mass planets would have formed by planetesimal accretion, very similar to the way the Earth was formed, rather than by the processes which are responsi-

ble for the formation of gas giant planets (of a few hundred M_{\oplus}). Clearly the detection of these kind of planets would be of special interest for future space missions which will be dedicated to search for Earth analogs (KEPLER, NASA's TPF & ESA's Darwin).

After the first year of the project the size of our target sample is still insufficient to arrive at any significant statistical conclusions, but we constantly add new targets to our list and the extension of our survey, both in target numbers as well as in time, will allow us in the future to determine useful quantitative limits for planets around M-dwarf stars.

We are grateful to the McDonald Observatory TAC for generous allocation of observing time. The help and support of the HET staff and especially of the resident astronomers, Matthew Shetrone, Brian Roman and Jeff Mader were also crucial for this project. We thank the referee for her/his helpful comments which improved the manuscript. We would also like to thank Sebastian G. Els for kindly providing his proper-motion routine for the velocity correction to the Solar System barycenter. Barbara McArthur and G. Fritz Benedict helped with many valuable discussions on M-dwarf binarity (moreover, Fritz helped with two sailing trips). We also thank Günter Wuchterl and Jack Lissauer for helpful discussions on planet formation around M-dwarfs. This material is based upon work supported by the National Aeronautics and Space Administration under Grant NAG5-9227 issued through the Office of Space Science, and by National Science Foundation Grant AST-9808980.

REFERENCES

- Benedict, G.F., et al. 2002, ApJ, 581, L115
- Boss, A.P. 1997, Science, 276, 1836
- Butler, R.P., Marcy, G.W., Williams, E., McCarthy, C., Dosanji, P., & Vogt, S.S. 1996, PASP, 108, 500
- Cochran, W.D., Hatzes, A.P., & Paulson, D.B. 2002, AJ, 124, 565
- Cochran, W.D., Tull, R.G., MacQueen, P.J., Paulson D.B., Endl, M. & Hatzes, A.P. 2003, in ASP Conf. Ser., Vol. 294, 561, ed. D. Deming & S. Seager
- Delfosse, X., Forveille, T., Mayor, M., Perrier, C., Naef, D., & Queloz, D. 1998, A&A, 338, L67
- Delfosse, X., Forveille, T., Beuzit, J.-L., Udry, S., Mayor, M., & Perrier, C. 1999, A&A, 344, 897
- Endl, M., Kürster, M., & Els, S. 2000, A&A, 362, 585
- Endl M., Kürster M., Rouesnel F., Els S., Hatzes A.P., & Cochran W.D., 2003, in ASP Conf. Ser., Vol. 294, 75, ed. D. Deming & S. Seager
- ESA 1997, The Hipparcos and Tycho Catalogues, ESA SP-1200
- Fischer, D.A., Marcy, G.W., Butler, R.P., Vogt, S.S., Henry, G.W., Pourbaix, D., Walp, B., Misch, A.A., & Wright, J.T., 2003, ApJ, 586, 1394
- Franz, O.G., et al. 1998, AJ, 116, 1432
- Gliese, W., & Jahreiß, H. 1991, Preliminary Version of the Third Catalogue of Nearby Stars, Astronomical Data Center CD-ROM
- Harrington, R.S. 1977, PASP, 89, 214
- Hünsch, M., Schmitt, J.H.M.M., Sterzik, M.F., & Voges, W. 1999, A&ASS, 135, 319
- Kürster, M., Endl, M., Rouesnel, F., Els, S., Kaufer, A., Brilliant, S., Hatzes, A.P., Saar, S.H., & Cochran, W.D. 2003, A&A, in press
- Lippincott, L.S., & Borgman, E.R. 1978, PASP, 90, 226
- Lomb, N.R. 1976, Ap&SS, 39, 477
- Marcy, G.W., Butler, R.P., Vogt, S.S., Fischer, D., & Lissauer, J.J. 1998, ApJ, 505, L147
- Marcy, G.W., Butler, R.P., Fischer, D., Vogt, S.S., Lissauer, J.J., & Rivera, E.J. 2001, ApJ, 556, 296
- Mayor, M., & Queloz, D., 1995, Nature, 378, 355
- Nakano, T. 1988, MNRAS, 235, 193

Nidever, D.L., Marcy, G.W., Butler, R.P., Fischer, D.A. & Vogt, S.S. 2002, ApJS, 141, 503

Pollack, J.B., Hubickyj, O., Bodenheimer, P., Lissauer, J.J., Podolak, M., & Greenzweig, Y. 1996, Icarus, 124, 62

Scargle, J.D. 1982, ApJ, 263, 835

Tokovinin, A.A. 1992, A&A, 256, 121

Tull, R.G. 1998, Proc SPIE Vol. 3355, 387

Vogt, S.S., Marcy, G.W., Butler, R.P., & Apps, K. 2000, ApJ, 536, 902

Wetherill, G.W. 1996, Icarus, 119, 219

Star	Sp.T.	V [mag]	N	rms [m s ⁻¹]	ΔT [days]
GJ 2	M2V	9.93	5	2.6	20
GJ 87	M2.5V	10.06	5	8.8	40
GJ 155.1	M1V	11.04	5	6.1	16
GJ 184	M0V	9.93	5	7.3	41
GJ 192	M3.5V	10.76	3	3.5	4
GJ 3352	M3V	11.07	6	5.0	23
GJ 251.1	M1.5V	10.55	6	13.0	16
GJ 272	M2V	10.53	5	4.0	7
GJ 277.1	M0V	10.49	6	8.7	14
GJ 281	M0V	9.61	4	6.6	15
GJ 289	M2V	11.46	5	7.6	52
GJ 308.1	M0V	10.33	8	12.4	40
GJ 310	M1V	9.30	7	15.9	71
GJ 328	M1V	9.99	5	6.2	42
GJ 353	M2V	10.19	5	9.4	10
GJ 378	M2V	10.07	5	4.6	7
GJ 411	M2Ve	7.48	23	7.2	380
GJ 2085	M1V	11.18	5	6.2	10
GJ 436	M3.5V	10.67	17	20.6	394
GJ 535	M0V	9.03	5	3.0	27
GJ 552	M2.5V	10.68	6	11.3	33
GJ 563.1	M2V	9.71	6	4.9	24
GJ 623*	M3V	10.28	11	5.0	116
GJ 671	M3V	11.37	7	6.1	12
GJ 687	M3.5V	9.18	5	2.9	10
GJ 699	M4V	9.53	16	7.2	36
GJ 708	M1V	10.07	6	9.2	23
GJ 4070	M3V	11.27	6	8.0	60
GJ 731	M1.5V	10.15	4	3.4	6
GJ 748*	M4V	11.10	7	5.5	26
GJ 839	M1V	10.35	6	6.3	14
GJ 849	M3.5V	10.37	4	1.2	34
GJ 864*	M1V	10.01	9	7.3	31
GJ 895	M2Ve	10.04	5	3.8	5
GJ 913*	M0.5V	9.62	5	6.5	19

Table 1: Radial velocity results for 35 M-dwarfs (4 variable M-dwarfs of our program are not listed here). Spectral classification and visual magnitudes are taken from the Gliese catalogue, N is the total number of obtained RV measurements, rms is the total scatter of the RVs and ΔT denotes the duration of monitoring (i.e. the time span from first to last observation of this star). Notes: for the 4 stars marked with an asteriks the rms is given after subtraction of an RV-trend (see section 3.3).

This 2-column preprint was prepared with the AAS L^AT_EX macros v5.0.

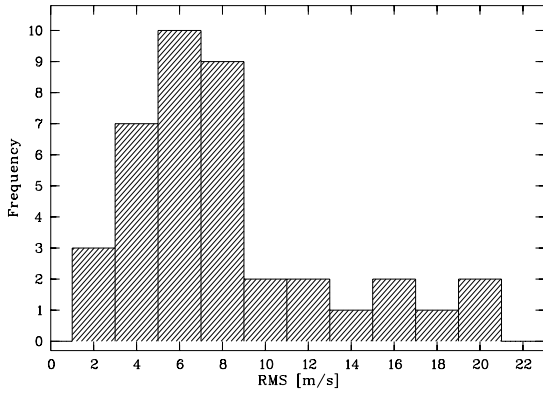


Fig. 1.— Histogram of the HET/HRS RV-results for 39 M-dwarfs from our sample. The left-hand side contains constant stars and targets which show no excess residual signal after subtraction of RV-trends. Fitting a gaussian to this part of the histogram yields a mean RV-scatter of 5.7 m s^{-1} and $\sigma = 2.2 \text{ m s}^{-1}$. The right-hand “tail” of the distribution consists of more variable stars with rms-values higher than 10 m s^{-1} .

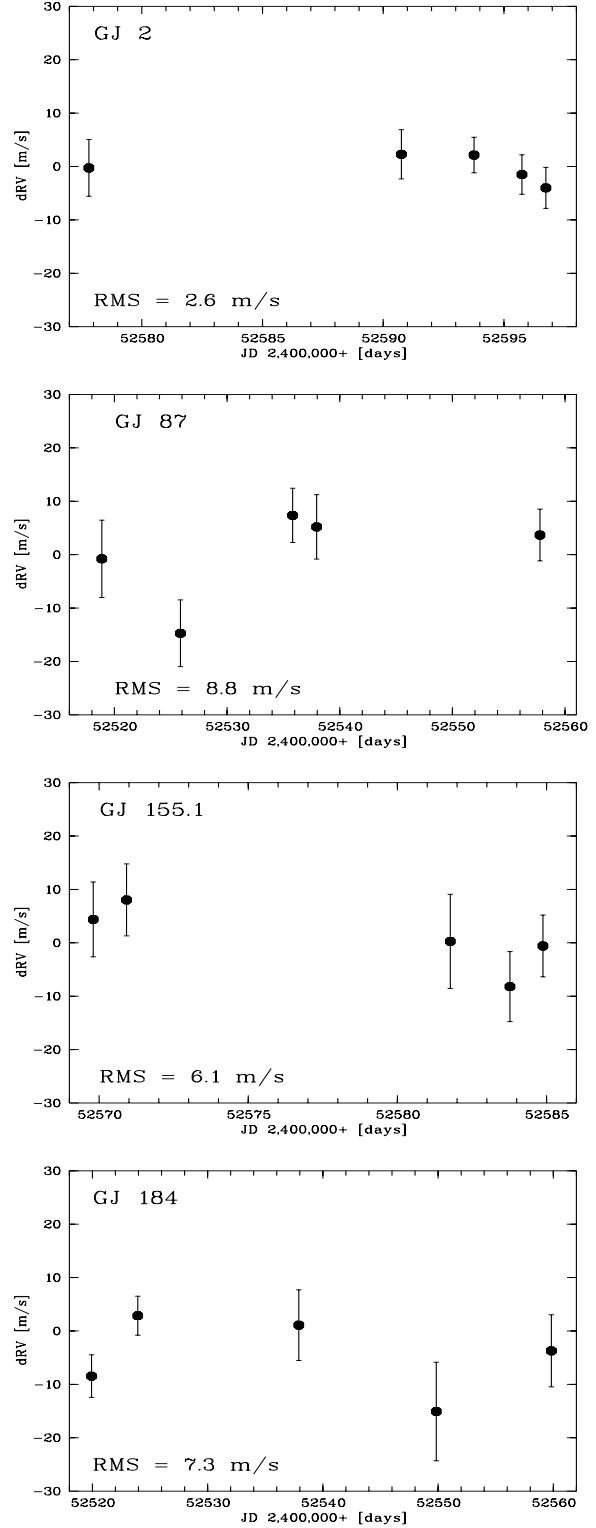


Fig. 2.— RV results for GJ 2, GJ 87, GJ 155.1 and GJ 184.

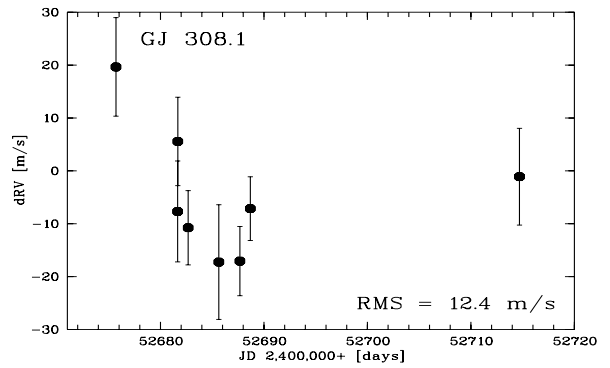
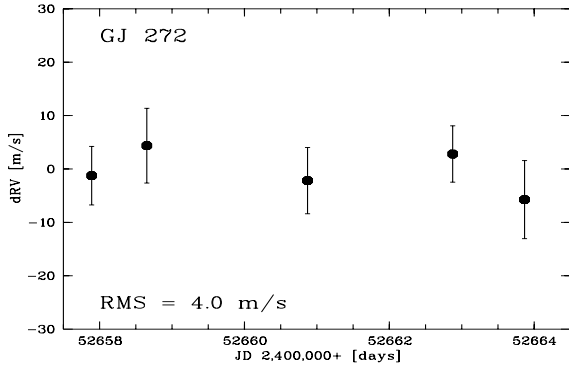
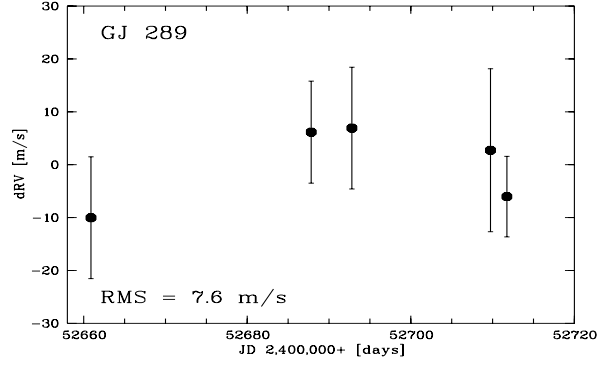
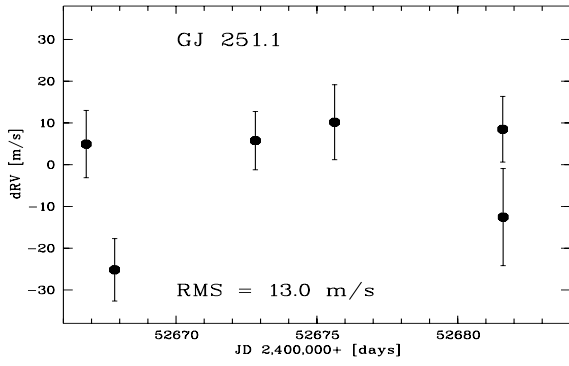
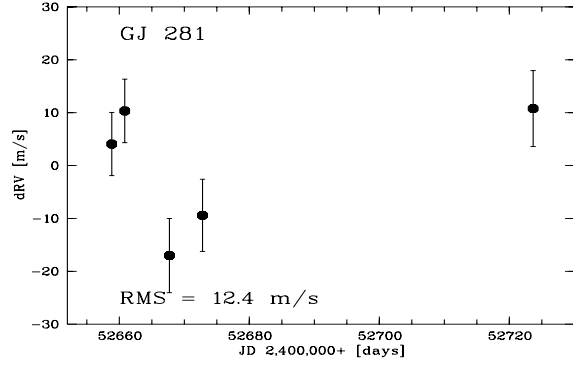
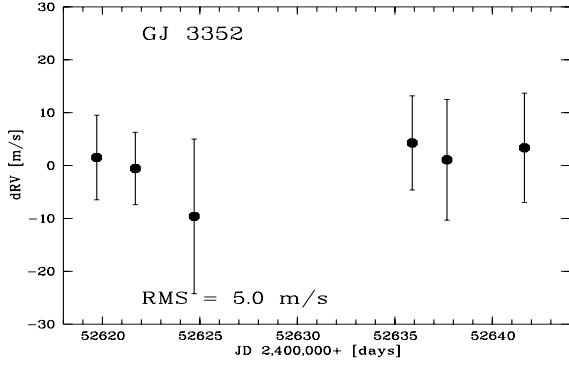
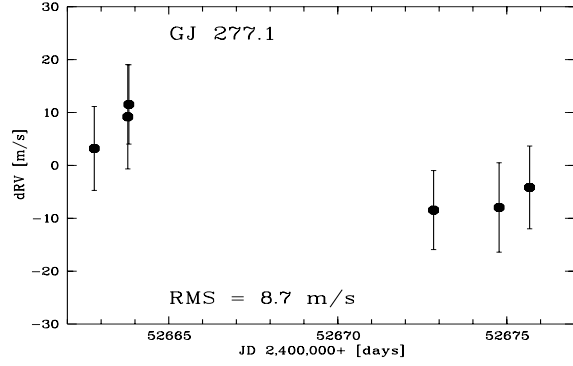
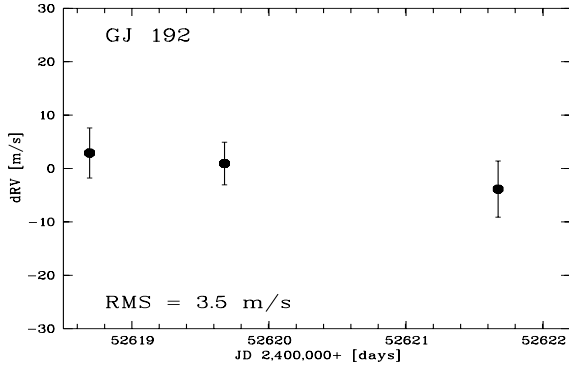


Fig. 3.— RV results for GJ 192, GJ 3352, GJ 251.1, and GJ 272.

Fig. 4.— RV results for GJ 277.1, GJ 281, GJ 289, and GJ 308.1.

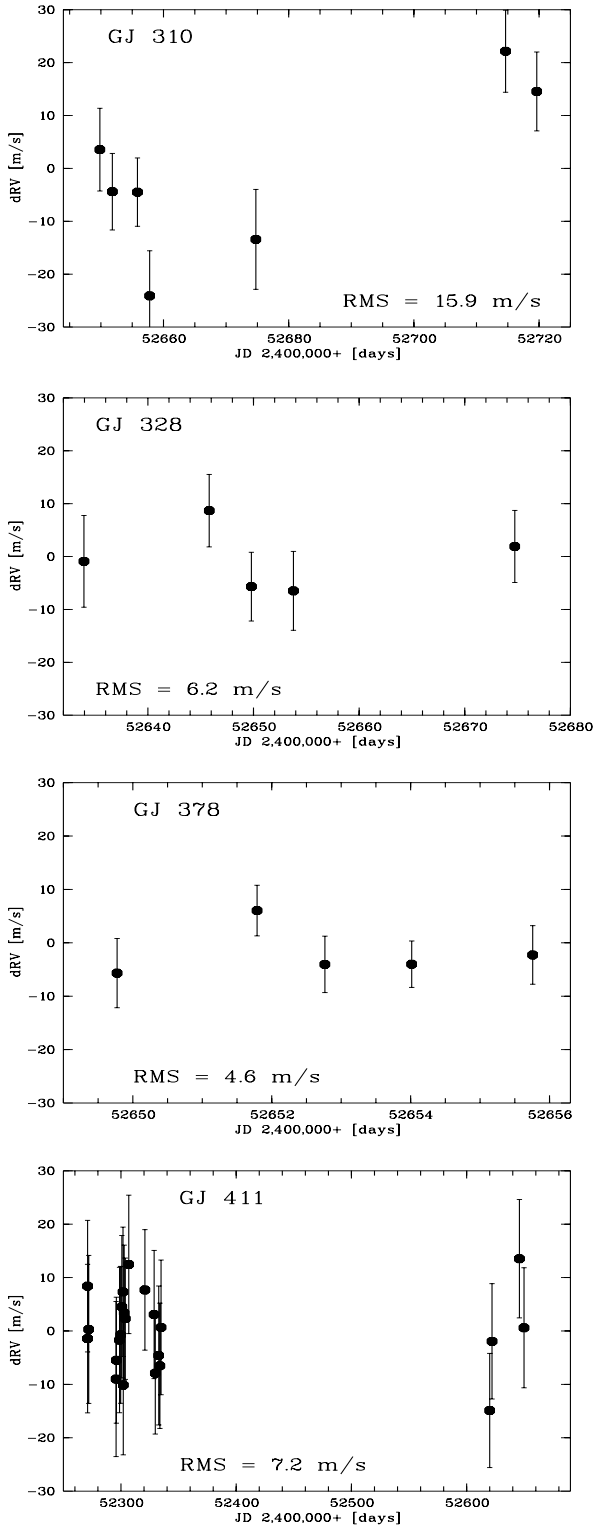


Fig. 5.— RV results for GJ 310, GJ 328, GJ 353, GJ 378, and GJ 411

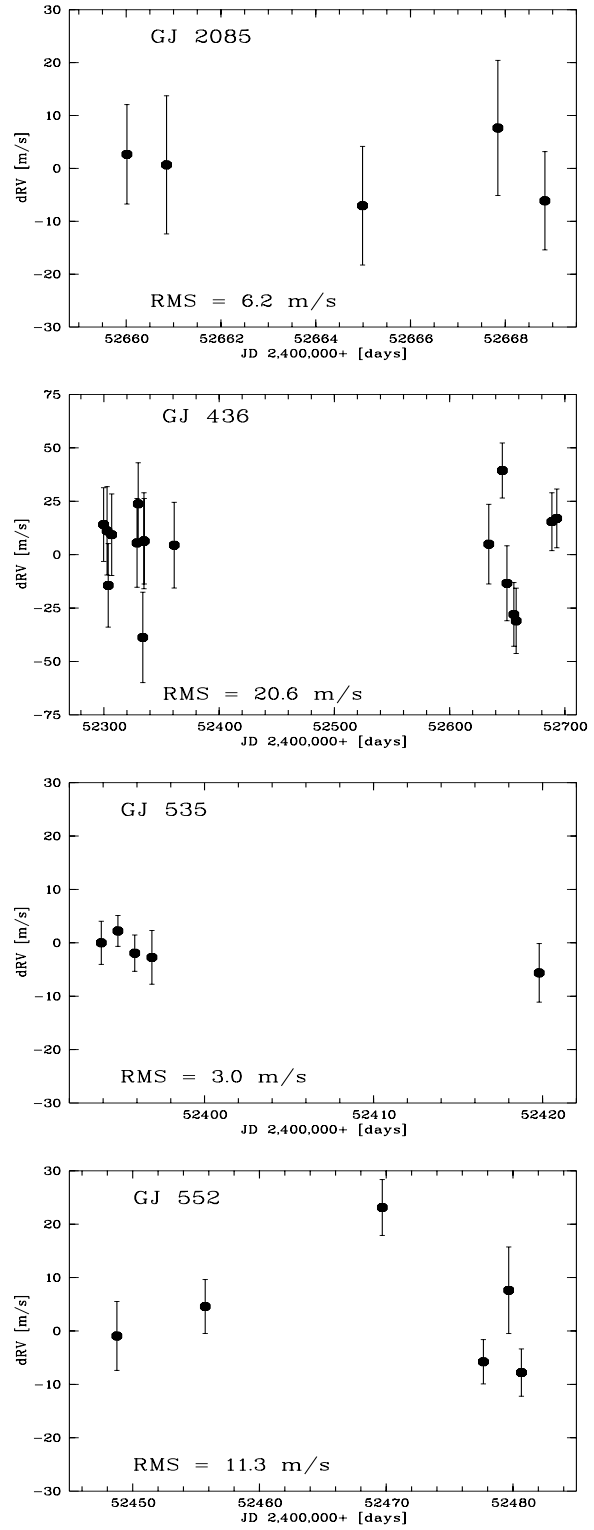


Fig. 6.— RV results for GJ 2085, GJ 436 (note the larger velocity scale), GJ 535, and GJ 552.

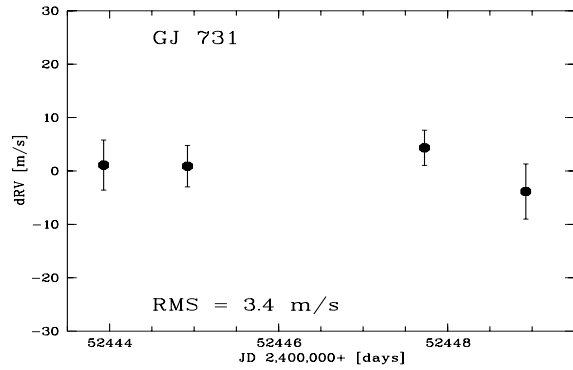
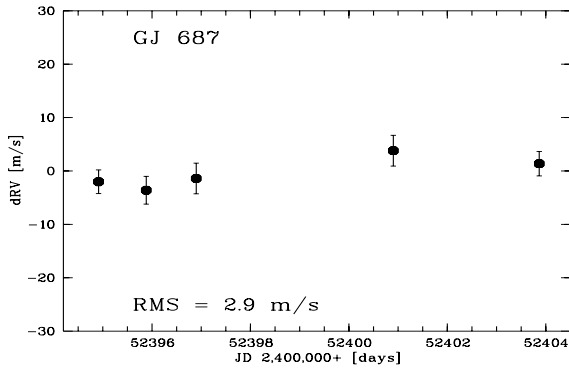
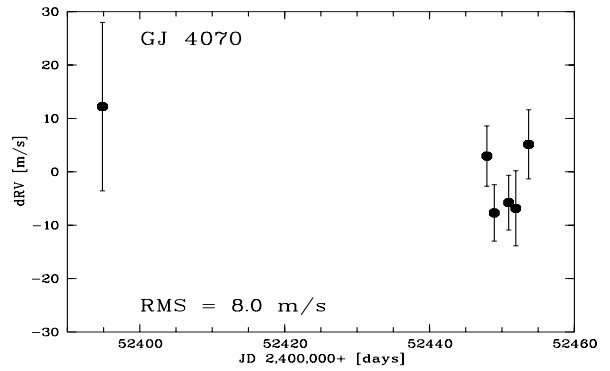
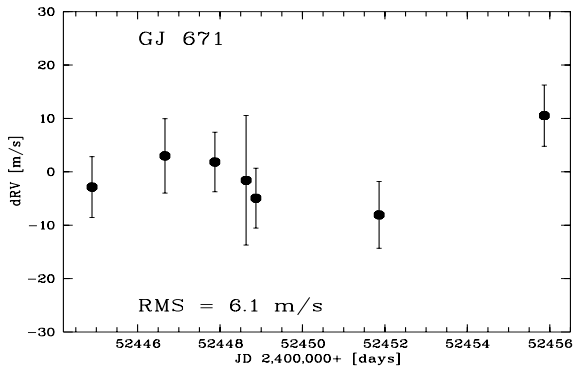
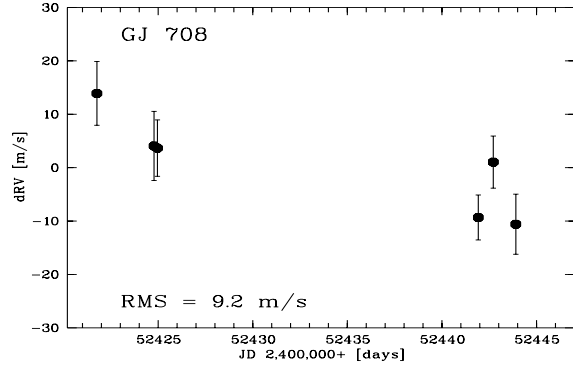
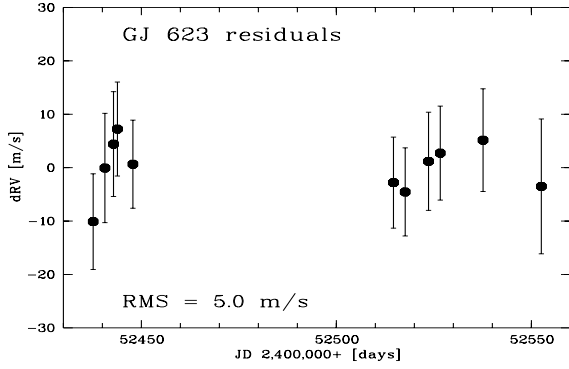
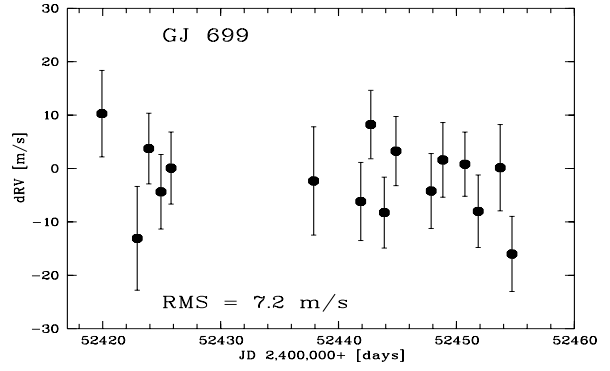
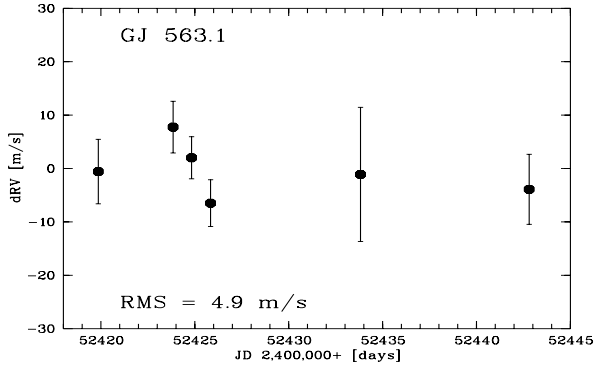


Fig. 7.— RV results for GJ 563.1, GJ 623 (residuals), GJ 671, and GJ 687

Fig. 8.— RV results for GJ 699, GJ 708, GJ 4070, and GJ 731.

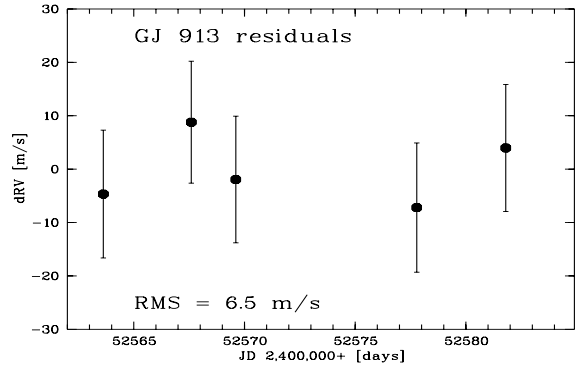
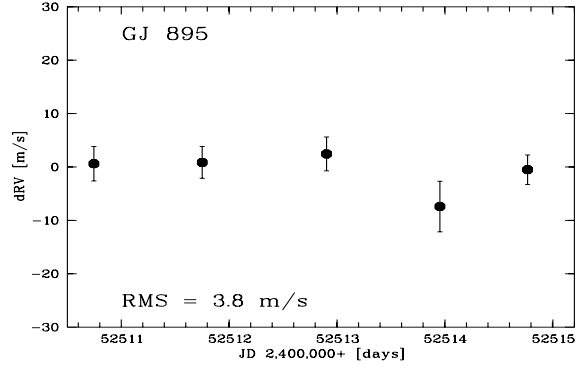
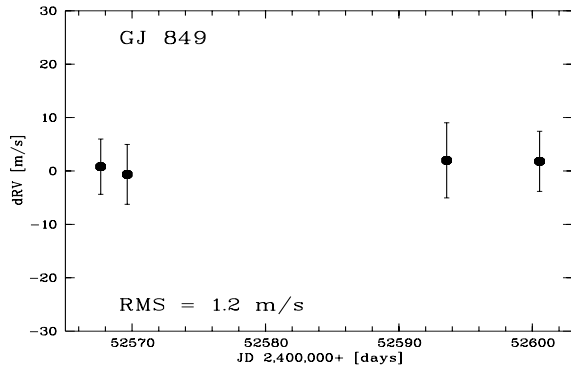
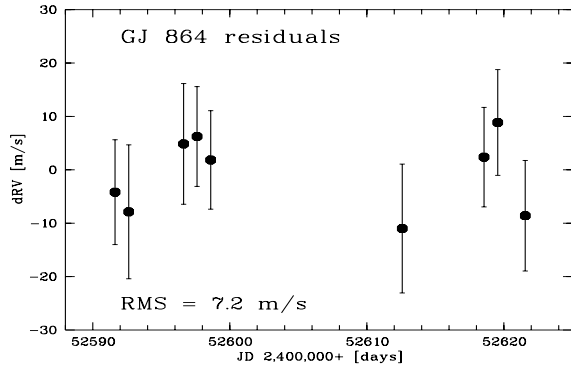
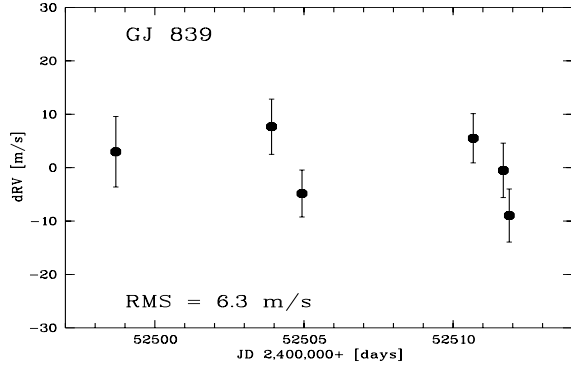
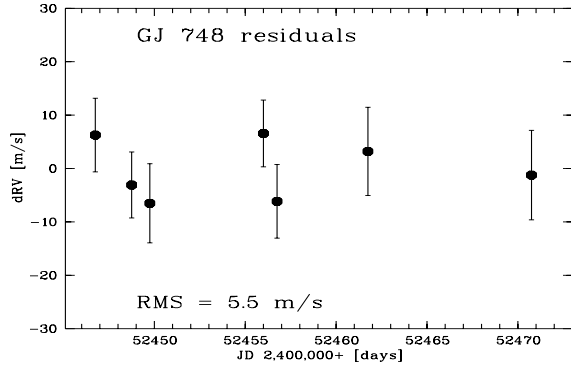


Fig. 10.— RV results for GJ 895 and GJ 913 (residuals).

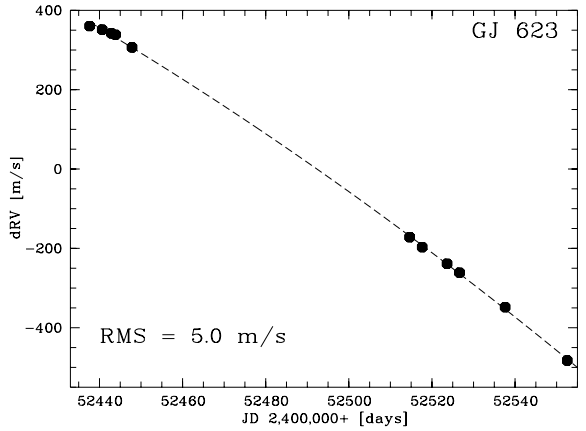


Fig. 11.— HET RV-data for the known binary GJ 623 showing a part of the binary orbit. The rms scatter around the best-fit parabolic trend is 5.0 m s^{-1} (see Fig. 7 for the residuals).

Fig. 9.— RV results for GJ 748 (residuals), GJ 839, GJ 864 (residuals), and GJ 849.

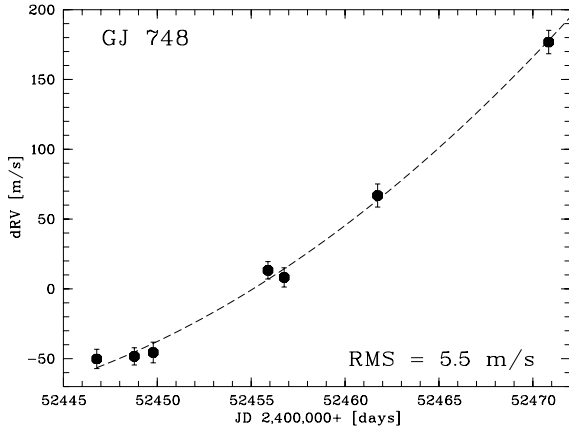


Fig. 12.— HET RV-data for the binary GJ 748 showing a small fraction of the binary orbit ($P = 2.45$ yrs). The rms scatter around the best-fit parabolic trend is 5.5 m s^{-1} (see Fig. 8 for the residuals).

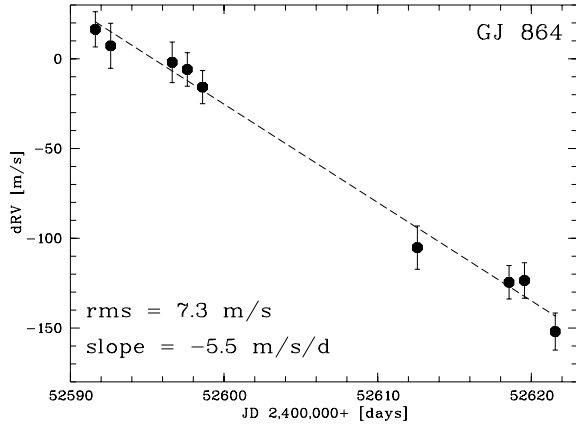


Fig. 14.— HET RV-data of GJ 864 showing a linear acceleration of $-5.5 \text{ m s}^{-1} \text{ d}^{-1}$. The rms-scatter around this trend is 7.3 m s^{-1} . Using additional observations with the McDonald 2.7 meter telescope we confirmed that the linearity of this trend continued until January 2003 and that the best explanation is a previously unknown stellar companion at yet undetermined separation.

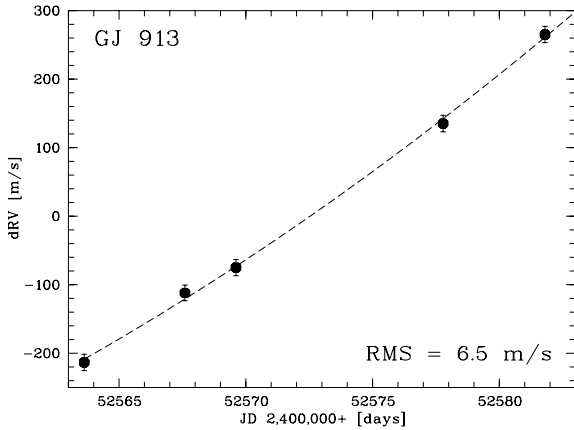


Fig. 13.— GJ 913, a Hipparcos candidate for a short-period binary system, shows a large amplitude RV variation indicative of a stellar companion. The rms scatter around the best-fit parabolic trend is 6.5 m s^{-1} (see Fig. 9 for the residuals). Further observations might allow us to determine a spectroscopic orbital solution.